Slot-Enhanced Dual-Band Microstrip Ring Resonator Sensor for Non-Invasive Blood Glucose Measurement

Amjad Hussein Yousif, Saad Wasmi Osman Luhaib, and Mohammed Younis Thanoun

Abstract—This paper presents a new solt-enhanced dual-band microstrip ring resonator for non-invasive glucose estimation fabricated on FR-4. The slot placed beneath the sample to increase electric-field participation in the sensing volume. The structure supports two well-separated resonances near 2.4 GHz and 5 GHz whose minima shift monotonically with glucose concentration across 0–400 mg/dL, enabling linear inverse modeling and ratio metric features that mitigate common-mode drift. Five regression models were evaluated—single-band linear and quadratic (for each band) and a dual-band linear mapping using (f1,f2)—on a dataset generated with a Debye-based permittivity parameterization; the dual-band linear model delivered the best accuracy–robustness trade-off with training MAE = 8.53 mg/dL, RMSE = 10.13 mg/dL, R^2=0.9938, and leave-one-out cross-validation R^2=0.9881, MAE = 12.23 mg/dL, RMSE = 14.11 mg/dL, whereas a quadratic dual-band alternative over fit. Frequency-detection resolution and normalized sensitivity are reported for both bands to support fair comparison among configurations, and the slot-enhanced layout achieves higher sensitivity without sacrificing compactness, indicating a practical path toward calibration-efficient bio sensing.

Index Terms—Dual-band resonator; FR-4; Microwave bio sensing; Non-invasive glucose; Slot-enhanced coupling.

I. INTRODUCTION

DIABETES now impacts more than 8% of the global population, heightening demand for accurate, painless monitoring of blood glucose levels (BGL) [1]. Continuous, non-invasive blood-glucose monitoring has become a priority in healthcare technology because invasive electro-chemical methods still suffer from discomfort, calibration drift, and limited real-time capability. Microwave sensing provides a promising alternative thanks to its ability to penetrate biological tissue and correlate dielectric variations with glucose concentration. Nevertheless, most reported microwave sensors exhibit single-band operation, narrow dynamic range, or complex fabrication that limits practical deployment. Routine finger-stick assays,

though ubiquitous, are invasive, inconvenient, and raise cross-infection concerns in shared settings, which can reduce adherence over time [2]. Numerous optical noninvasive methods have been explored, but their reliability is often curtailed by modest signal-to-noise ratios and vulnerability to calibration drift, temperature, and ambient humidity [3]. System-level design and frequency-domain characteristics have a decisive impact on the stability and reliability of microwave systems. Prior studies reported in [4] and [5] indicate that careful architectural optimization, together with the use of multiple operating frequencies, leads to more stable and repeatable performance, particularly in compact planar configurations. As an alternative, microwave sensing leverages the dependence of complex permittivity on glucose concentration and can be realized with compact, planar structures compatible with standard microwave circuitry [6], [7]. Field-confining resonant and transmission-line architectures localize the electric field within a designated sensing region, boosting sensitivity while maintaining straightforward fabrication and integration [8], [9]. Prior studies—including dual-mode resonators and split-ring resonators (SRR) and complementary split-ring resonators (CSRR)-based implementations—substantiate the feasibility of microwave biosensing for glucose tracking and motivate continued advances in linearity, robustness, and calibration methodologies [10]-[12].

The main contributions of this paper are summarized as follows:

- Combining a compact slot-enhanced field-confinement mechanism with dual-band ring resonator to design and simulate on an FR-4 substrate ($\varepsilon_r = 4.4$, $h = 1.6$ mm), exhibiting well-separated resonances near 2.4 and 5 GHz.
- The integration of a narrow sub-sample slot beneath the sensing cylinder enhances electric field coupling and significantly improves sensitivity.
- Debye-based dielectric modeling of glucose–water mixtures (0–400 mg/dL) is simulated to achieve high prediction accuracy.
- Five regression models (linear/quadratic single-band and dual-band) are evaluated with cross-validation to determine the optimal frequency–concentration mapping.
- Comparative analysis with recent state-of-the-art sensors demonstrates superior sensitivity (1 MHz/(mg/dL)) and manufacturability on a low-cost FR-4 substrate.

In this context, our dual-band sensor aims to achieve higher

frequency-shift sensitivity per mg/dL compared to previous dual-band reports. It specifically addresses linearity in the range of 0–400 mg/dL and enhances packaging for stable coupling. Two resonances near ISM bands are utilized for cross-validation and drift rejection. Additionally, a fine slot located beneath the sample cylinder concentrates the electric field within the sensing region, thereby increasing the frequency shift per mg/dL and promoting linearity in both bands.

This paper is organized as follows. Section II reviews related work on non-invasive microwave glucose sensors. Section III presents the proposed sensor design, equivalent model, and parametric optimization. Section IV describes the simulation setup, dataset generation, and performance evaluation, including comparison with other methods. Finally, Section V concludes the paper and outlines directions for future research.

II. RELATED WORK

Numerous microwave sensor architectures have been explored for non-invasive glucose measurement. Early planar resonators such as single open-loop and patch cavities [1], [2], [3]demonstrated the feasibility of correlating the resonant-frequency shift with blood-glucose concentration. However, their single-band nature limited the sensing range and accuracy.

Recent dual-band designs aim to exploit field localization at two resonances to improve robustness and dynamic range for non-invasive BGL estimation. Farouk et al. proposed a dual-band band-pass transmission-line sensor operating near 2.45/5.2 GHz, reporting successful glucose discrimination on phantoms and arguing that two bands mitigate single-band ambiguities; however, the study still relied on controlled setups with limited subject variability and did not fully quantify per-mg/dL frequency-shift sensitivity across clinically relevant ranges [13].

Kandwal et al. introduced an enclosed split-ring, metamaterial-based array that exhibits two resonances and emphasizes compactness and coupling stability, yet the evaluation emphasized solution measurements and device footprint more than rigorous FDR (MHz/(mg/dL)) benchmarking, leaving open questions on calibration drift and on-body coupling repeatability [14]. On-body resonant platforms have also advanced:Soltanian et al. demonstrated a high-FoM plasmonic microwave resonator measured around 3.25 and 4.67 GHz, highlighting wearability but noting the need to decouple contact pressure and tissue coupling from permittivity-driven glucose effects [15].

Beyond specifically dual-band layouts, work on resonator-based biosensors has reported MHz-per-mg/dL-level sensitivities on liquid glucose models—e.g., Yue et al. achieved 1.38 MHz/(mg/dL) over 25–300 mg/dL with careful field focusing—yet translation to on-body, non-contact use remains limited by placement repeatability and subject-to-subject variability [16]. Foundational demonstrations such as Choi et al. (microwave noninvasive topology with interference testing) and the chipless SRR tag of Baghelani et al. underscore feasibility and continuous-monitoring potential but also document calibration drift, hydration-related confounders, and small-cohort validations as persisting constraints [10]-[12].
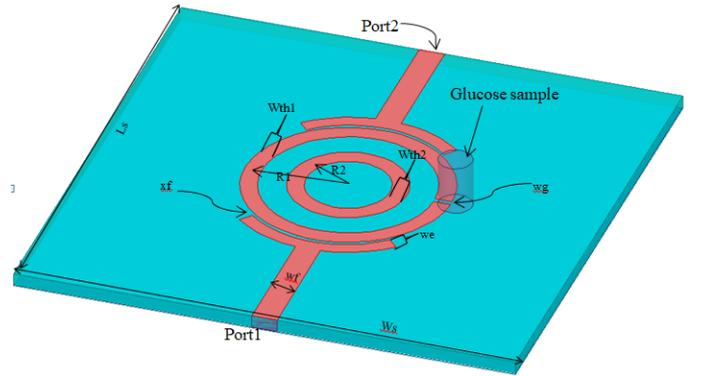

Fig. 1. Schematic of dual-band ring resonator sensor for non-invasive glucose.

III. SENSOR DESIGN AND EQUIVALENT MODEL

Fig. 1 shows the new proposed dual mode resonators non-invasive glucose measured. The front layer design comprises two concentric microstrip rings side-coupled to a 50-Ω feed over a continuous ground plane on FR-4 substrate with ϵ_r=4.4 ,the height is 1.6mm and the tanδ=0.02. In the slot-enhanced configuration, a microstrip slot is introduced under the cylinder (material under test) placed at a high-$|E|$ sector. The dimensions of cylinder tester were 4mm for a diameter and 6mm for height. The material under test (MUT) is considered as an aqueous medium with dielectric characteristics that vary according to glucose concentration, serving as a blood-equivalent representation. The dependence of the complex permittivity on glucose concentration is modeled using a Debye-type dispersion formulation. This approach allows resonance frequency variations to be analyzed under controlled conditions, while minimizing the influence of external experimental uncertainties.The input feeding was realized by electric coupling which depend on the length of arc (Lr) and the gap (xf) For sizing the dual-band microstrip ring resonator, use the resonance relation [17]:

$$f_r = \frac{n\,c}{2\pi\,r_{\mathrm{mean}}\sqrt{\varepsilon_{\mathrm{eff}}}} \qquad (1)$$

where f_r is the target resonance (2.4 GHz or 5 GHz), n is the mode index (typically n = 1 for the fundamental), $c = 3108m/s is the speed of light$, r_{mean} is the ring's mean radius, and ϵ_{eff} is the effective dielectric constant set by the substrate and microstrip geometry. Rearranging gives the practical design rule[17]:

$$r_{\mathrm{mean}} = \frac{n\,c}{2\pi\,f\,\sqrt{\varepsilon_{\mathrm{eff}}}} \qquad (2)$$

which directly links the desired frequency to ring size; the 5 GHz ring is roughly half the radius of the 2.4 GHz ring if ϵ_{eff} is the same. In practice, compute ϵ_{eff} from the chosen stack-up (substrate ϵ_r, thickness) and line width using a standard microstrip model, then fine-tune ring width and coupling gaps in full-wave simulation to place the modes precisely at 2.4 and 5 GHz.

Table I illustrates the dimensions of the proposed sensor that get from equations 1 and 2 and optimization by Hfss software

TABLE I
DIMENSIONS OF THE PROPOSED DUAL-MODE SENSOR CONFIGURATION

Dimensions	Value
Substrate width W_s	60 mm
Substrate length L_s	60 mm
Substrate thickness h_s	1.6 mm
Outer ring radius R_1	11.3 mm
Outer ring strip width W_{th1}	2 mm
Inner ring radius R_2	8 mm
Inner ring strip width W_{th2}	2 mm
Feed line width W_f	3 mm
Feed line length extension L_f	5 mm
Feed line extension width W_e	1.7 mm
Gap (feed to outer ring) X_f	0.15 mm
Glucose cylinder radius r_c	2 mm
Glucose cylinder height h_c	6 mm
Cylinder center offset cen_1	0.5 mm
Slot width in outer ring W_g	0.18 mm

Fig. 2. Frequency response (S_{11}) for the proposed sensor.

The sample test was simulated by Debye equation as follow [18]:

$$\varepsilon_r(\omega, C_x) = \varepsilon_\infty(C_x) + \frac{\varepsilon_{\text{stat}}(C_x) - \varepsilon_\infty(C_x)}{1 + j\,\omega\,\tau(C_x)} \quad (3)$$

where C_x is glucose concentration in mg/dL; ω is angular frequency in rad/s; $\varepsilon_\infty(C_x)$ is the high-frequency permittivity; $\varepsilon_{\text{stat}}(C_x)$ is the static permittivity; $\tau(C_x)$ is the molecular relaxation time in seconds.

$$\varepsilon_\infty(C_x) = 5.38 + 0.003\, C_x \quad (4)$$

$$\varepsilon_{\text{stat}}(C_x) = 80.68 - 0.0207\, C_x \quad (5)$$

$$\tau(C_x) = \left(9.68 + 0.023\, C_x\right) \times 10^{-12}\ \text{s} \quad (6)$$

IV. MEASUREMENT SETUP, DATASET, AND ANALYSIS

Fig. 2 shows the simulated magnitude of the reflection coefficient S_{11} for the proposed dual-band resonator over 0-6 GHz with the under-test medium being deionized water (0 mg/dL glucose). Two well-separated notches are observed at f1 = 2.244 GHz (minimum $S_{11} \approx$ -17.8 dB) and at f2 = 4.672 GHz (minimum $S_{11} \approx$ -15.0 dB), as marked. These frequencies can be changed by the concentrate of glucose level in sample test.

Fig. 3 displays the simulated frequency response for dual-band ring resonator non-invasive glucose level measurement at different concentrations of glucose. It can be seen that there are dual-band frequencies with readable values for the S parameter in each band. It is highly effective in terms of frequency when the glucose level is changing. For band 1, the frequency changes from 2.54 GHz to 2.694 GHz when the concentration increases from 0 to 200 mg/dL. On the other hand, band two experiences a frequency change from 5.078 GHz to 5.268 GHz under the same conditions.

Fig. 4 plots the extracted resonance frequencies of the dual-band ring resonator versus glucose concentration from 0 to
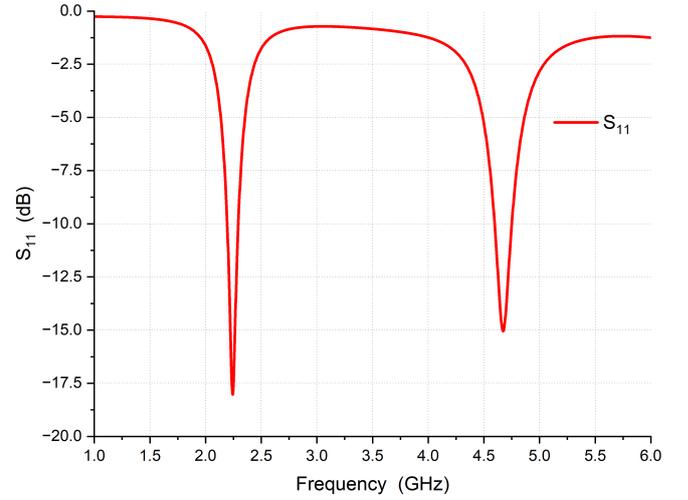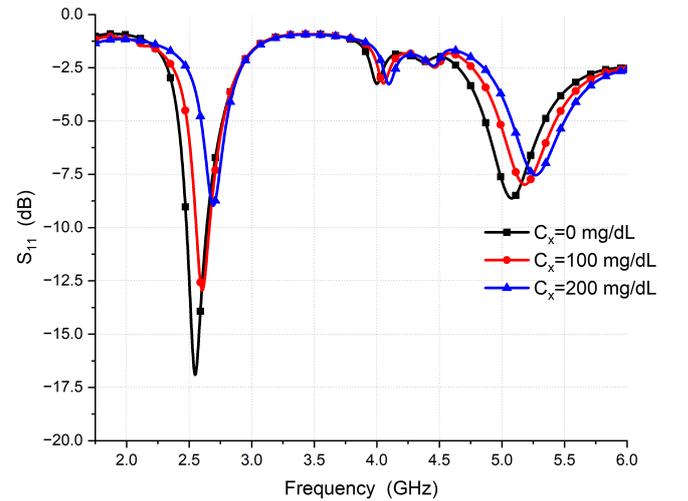

Fig. 3. The frequency response of sensor under various glucose levels.

400 mg/dL. Both modes shift monotonically upward with concentration: the lower-band resonance f_1 increases from ≈ 2.54 to ≈ 2.96 GHz ($\Delta \approx 0.42$ GHz), corresponding to an average sensitivity of ≈ 1.0–1.1 MHz/(mg/dL), whereas the upper-band resonance f_2 rises from ≈ 5.10 to ≈ 5.37 GHz ($\Delta \approx 0.27$ GHz), yielding ≈ 0.7–0.8 MHz/(mg/dL). The steeper slope of f_1 indicates stronger field overlap with the sample and thus higher sensitivity at the lower band. A mild change in the f_2 slope around 150–200 mg/dL is also evident, consistent with concentration-dependent dispersion in the Debye parameters.

Several curve fittings have been applied to the data gates by changing the frequencies as a function of constriction to improve glucose level estimation.

Table II summarizes inverse regression models that map the resonant minima f_1 and f_2 (GHz) to glucose concentration C_x (mg/dL). We report training R^2, mean absolute error (MAE), root-mean-square error (RMSE), and maximum absolute error ($\max|err|$); for dual-band models we

TABLE II
RESULTS OF DIFFERENT CURVE-FITTING METHODS

Category	Model	Train			LOOCV	
		R^2	MAE	Error	R^2	MAE
Single-band	Linear (f1)	0.968	22.96	36.13	0.93	27.40
Single-band	Quadratic (f1)	0.994	10.08	23.08	0.99	12.66
Single-band	Linear (f2)	0.950	28.77	51.29	0.91	30.63
Single-band	Quadratic (f2)	0.979	18.50	34.02	0.93	28.24
Dual-band	Linear (f1,f2)	0.994	10.13	17.77	0.99	12.23

TABLE III
FDR AND NORMALIZED SENSITIVITY FOR EACH CURVE-FITTING MODEL

Category	Model	FDR (mg/dL/GHz)	S (1/mg/dL)
Single-band (f_1)	Linear	1.113	0.0437
Single-band (f_1)	Quadratic	0.749	0.0294
Single-band (f_2)	Linear	0.833	0.0164
Single-band (f_2)	Quadratic	1.856	0.0365
Dual-band (f_1, f_2)	Linear	1.327	0.0230

also include leave-one-out cross-validation (LOOCV) metrics. Models were trained on nine concentrations spanning 0–400 mg/dL (50 mg/dL steps), with $f_1 \in [2.522, 2.963]$ GHz and $f_2 \in [5.044, 5.364]$ GHz. Among single-band fits, the quadratic model using f_1 achieved the best accuracy $\left(R^2_{\text{train}} = 0.9939,\ \text{MAE} = 8.13\ \text{mg/dL},\ \text{RMSE} = 10.08\ \text{mg/dL},\ \max|err| = 23.08\ \text{mg/dL}\right)$, outperforming both the f_1-linear model $\left(\text{MAE} = 19.93\ \text{mg/dL}\right)$ and f_2-based models (best: f_2-quadratic RMSE = 18.50 mg/dL). Leveraging both resonances improved generalization: the dual-band linear inverse,

$$C_x = -4053.913 + 524.410\, f_1 + 541.432\, f_2, \qquad (7)$$

achieved high fidelity in training $\left(\text{MAE} = 8.53\ \text{mg/dL},\ \text{RMSE} = 10.13\ \text{mg/dL},\ R^2 = 0.9938\right)$ and strong LOOCV performance $\left(R^2_{\text{LOOCV}} = 0.9881,\ \text{MAE} = 12.23\ \text{mg/dL},\ \text{RMSE} = 14.11\ \text{mg/dL}\right)$. By contrast, the dual-band quadratic model exhibited overfitting—excellent training error $\left(\text{MAE} = 5.34\ \text{mg/dL},\ \text{RMSE} = 6.91\ \text{mg/dL},\ R^2 = 0.9971\right)$ but degraded LOOCV $\left(R^2_{\text{LOOCV}} = 0.837,\ \text{RMSE} = 52.10\ \text{mg/dL}\right)$. Overall, the dual-band linear inverse provides the best accuracy–robustness trade-off and is recommended for calibration and deployment; the f_1-quadratic single-band model is a strong fallback when only one resonance is available. All errors are reported in mg/dL, frequencies in GHz, and LOOCV was used due to the small sample size ($n = 9$); extrapolation beyond 0–400 mg/dL
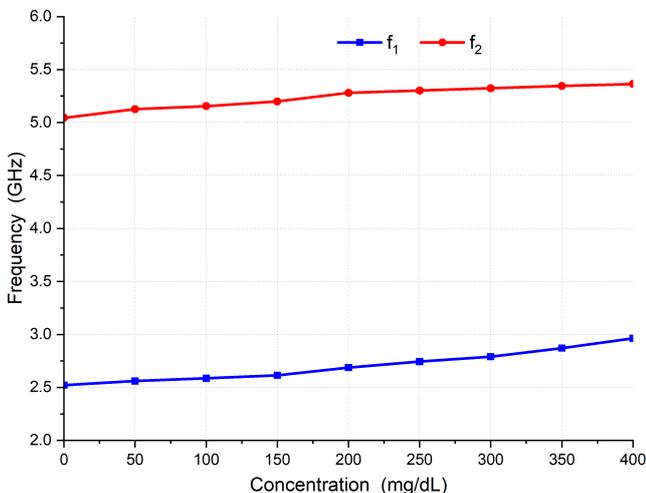
is not recommended. Another key metric is the frequency-detection resolution (FDR), expressed in $\text{MHz}/(\text{mg/dL})$, which can be obtained from the frequency–concentration sensors is the frequency-detection resolution (FDR), expressed in MHz/(mg/dL). The FDR can be determined as in [19]

$$\text{FDR}_i = \frac{\Delta f_i}{\Delta C_x} \qquad (8)$$

where Δf_i is the frequency shift of in frequency in each band, and ΔC_x is the variation of the glucose. Normalized sensitivity, reported in 1/(mg/dL), is used as the basis for fair sensor comparison [20][21].

$$S_i = \frac{\text{FDR}_i}{f_{i0}} \times 100 \qquad (9)$$

where f_{i0} is the frequency value at 0 mg/dL glucose consecration for band 1 and band 2.

The table III reports the frequency-detection resolution (FDR) in MHz/(mg/dL) and the normalized sensitivity (S) 1/(mg/dL) for five models: single-band linear and quadratic fits for f_1 and f_2, and a dual-band linear inverse model. The sensor shows the significant sensitivity for all models.

Table IV summarizes a detailed comparison between the proposed dual-band slot-enhanced sensor and several recently reported microwave glucose sensors. To ensure fairness, all results are normalized by substrate type, operating frequency, and measurement environment. A comparison with existing works shows that the proposed sensor offers a well-balanced combination of dual-band functionality, effective frequency-shift sensitivity, and practical implementation cost. In contrast to many previously reported sensors that rely on single-frequency operation, the proposed design operates at two resonant frequencies around 2.4 GHz and 5 GHz using a standard FR-4 substrate, with corresponding sensitivities of 1.05 MHz/(mg/dL) and 0.75 MHz/(mg/dL). The planar configuration and compact footprint further reduce fabrication complexity by avoiding multilayer structures or expensive substrate materials. Taken together, these characteristics position the proposed sensor as a practical and competitive approach for non-invasive microwave-based glucose monitoring.

V. CONCLUSION

A slot-enhanced dual-band microstrip ring resonator has been analyzed as a planar microwave sensor for non-invasive blood glucose monitoring. The proposed structure supports two well-separated resonant modes near 2.4 GHz and 5 GHz and is implemented on a standard FR-4 substrate, making it

Fig. 4. Resonant frequencies f1 and f2 versus glucose concentration (slot+cylinder).

TABLE IV
COMPARISON OF PROPOSED SENSOR WITH AVAILABLE BGL SENSORS

Ref.	Concentration (mg/dL)	f_0 (GHz)	S (MHz/(mg/dL))	S_n (1/(mg/dL))	MUT	Size (λ_g^2)
[20]	0–5000	4.18	0.026	6.2×10^{-4}	A.G.	0.016
[21]	70–120; 50–70	1.2	2×10^{-3}	N/A	A.G.	10.17
[22]	89–262	8.5; 5.5	3.58; 3.53	4×10^{-2}; 6×10^{-2}	Finger	0.5
[23]	75–150	8.8	1.5	1.7×10^{-2}	A.G.	1.5
[24]	0–500	1.016; 2.87	0.046; 0.5	4×10^{-3}; 1.7×10^{-2}	A.G.	0.001
[25]	0–1800	4.4725	0.0039	8.7×10^{-5}	A.G.	0.02
[26]	30–500	1.5	1.175	7.45×10^{-2}	A.G.	N/A
[27]	75–500	6.53	40.58	6.2×10^{-2}	A.G.	N/A
[28]	18–540	1.156	7.5×10^{-5}	6.48×10^{-6}	A.G.	0.02
[29]	N/A	3.5	N/A	3×10^{-2}	A.G.	N/A
[13]	0–200	2.45; 5.2	2.026; N/A	N/A	Phantom finger	0.288 at f1
[16]	25–300	0.8; 3.2	1.38	N/A	A.G./Serum	N/A
Proposed	0–400	2.54; 5.10	1.05; 0.75	0.0437; 0.0164	A.G.	0.697 (at f_1), 2.809 (at f_2)

Notes: MUT = material under test; A.G. = aqueous glucose solution; N/A = not available.

suitable for compact and low-cost realization. Full-wave electromagnetic simulations carried out in Ansys HFSS indicate that the introduction of a narrow slot beneath the sensing region modifies the local field distribution and increases electric-field concentration around the material under test, which in turn affects the resonant characteristics of the ring. Both resonant frequencies exhibit a monotonic and approximately linear shift with glucose concentration over the investigated range, with representative sensitivities of about 1.05 MHz/(mg/dL) at the lower band and 0.75 MHz/(mg/dL) at the higher band.

The presence of two independent resonant responses offers enhanced robustness against common-mode disturbances when compared to single-band configurations. These findings indicate that the proposed slot-enhanced dual-band resonator is a promising microwave sensing platform for further experimental exploration and the future advancement of non-invasive glucose monitoring systems.

REFERENCES

[1] International Diabetes Federation, "Diabetes facts & figures (IDF Diabetes Atlas 2025)," 2025. [Online]. Available: https://idf.org/

[2] Centers for Disease Control and Prevention, "Considerations for blood glucose monitoring and insulin administration," Aug. 7, 2024. [Online]. Available: https://www.cdc.gov/

[3] M. Shokrekhodaei and L. Quinones, "Review of non-invasive glucose sensing techniques," *Sensors*, vol. 20, no. 21, Art. no. 5936, 2020.

[4] B. J. Qeryaqos and S. A. Ayoob, "Proposed multiple reconfigurable intelligent surfaces to mitigate the inter-user-interference problem in NLOS," *Journal of Communications Software and Systems*, vol. 20, no. 3, pp. 245–252, 2024, doi: 10.24138/jcomss-2024-0039.

[5] H. A. Alsawaf and S. A. Ayoob, "Optimized wideband beamforming for mm-wave communication systems with intelligent reflecting surfaces," *Journal of Communications Software and Systems*, vol. 20, no. 4, pp. 350–360, Dec. 2024, doi: 10.24138/jcomss-2024-0090.

[6] T. Yilmaz, R. Foster, and Y. Hao, "Radio-frequency and microwave techniques for non-invasive measurement of blood glucose," *Sensors*, vol. 19, no. 4, Art. no. 800, 2019.

[7] J. Muñoz-Enano, V. E. Boria, and D. S. Passerini, "Planar microwave resonant sensors: A review and recent developments," *Applied Sciences*, vol. 10, no. 7, Art. no. 2615, 2020.

[8] R. A. Alahnomi, F. I. Ezeddin, A. A. Althuwayb, *et al.*, "Review of recent microwave planar resonator-based sensors: Techniques, challenges, and applications," *Sensors*, vol. 21, no. 8, Art. no. 2541, 2021.

[9] C. Liu, W. Zhao, and Q. Peng, "Microwave sensors and their applications in permittivity measurement: A review," *Micromachines*, vol. 15, no. 7, Art. no. 876, 2024.

[10] H. Choi, J. Naylon, S. Luzio, *et al.*, "Design and in vitro interference test of microwave noninvasive blood glucose monitoring sensor," *IEEE Trans. Microw. Theory Techn.*, vol. 63, no. 10, pp. 3016–3025, 2015.

[11] M. Baghelani, M. Sadeghikia, M. C. Eynon, and M. Daneshmand, "Non-invasive continuous-time glucose monitoring system using a chipless printable sensor based on split-ring microwave resonators," *Sci. Rep.*, vol. 10, Art. no. 12980, 2020.

[12] C. G. Juan, E. Vázquez, A. G. García, and Á. Lázaro, "Microwave planar resonant solutions for glucose concentration measurement: A review," *Applied Sciences*, vol. 11, no. 15, Art. no. 7018, 2021.

[13] M. Farouk, *et al.*, "Noninvasive blood glucose monitoring using a dual-band bandpass transmission-line sensor," *Scientific Reports*, 2025.

[14] A. Kandwal, *et al.*, "A dual-band microwave sensor for glucose measurements utilizing an enclosed split-ring metamaterial-based array," *Sensing and Bio-Sensing Research*, 2025.

[15] F. Soltanian, H. Afrand, R. C. Gupta, *et al.*, "On-body non-invasive glucose monitoring sensor based on a high-FoM plasmonic microwave resonator," *Scientific Reports*, 2023.

[16] W. Yue, H. Wang, J. Yang, *et al.*, "Permittivity-inspired microwave resonator-based biosensor," *Biosensors*, 2021. (Reports ~1.38 MHz/(mg/dL) on liquid glucose models.)

[17] J.-S. Hong and M. J. Lancaster, *Microstrip Filters for RF/Microwave Applications*. New York, NY, USA: Wiley, 2001.

[18] M. Hofmann, F. Trenz, R. Weigel, G. Fischer, and D. Kissinger, "A microwave sensing system for aqueous concentration measurements based on a microwave reflectometer," in *Proc. IEEE*, 2012.

[19] P. Mohammadi, A. Mohammadi, and A. Kara, "Dual frequency microwave resonator for non-invasive detection of aqueous glucose," *IEEE Sensors J.*, vol. 23, no. 18, pp. 21246–21253, 2023, doi: 10.1109/JSEN.2023.3303170.

[20] G. Govind and M. J. Akhtar, "Metamaterial-inspired microwave microfluidic sensor for glucose monitoring in aqueous solutions," *IEEE Sensors J.*, vol. 19, no. 24, pp. 11900–11907, Dec. 15, 2019.

[21] A. E. Omer, S. Gigoyan, G. Shaker, and S. Safavi-Naeini, "WGM-based sensing of characterized glucose–aqueous solutions at mm-waves," *IEEE Access*, vol. 8, pp. 38809–38825, 2020.

[22] S. Kiani, P. Rezaei, and M. Fakhr, "Dual-frequency microwave resonant sensor to detect noninvasive glucose-level changes through the fingertip," *IEEE Trans. Instrum. Meas.*, vol. 70, Art. no. 6004608, 2021.

[23] A. Kandwal et al., "Surface Plasmonic Feature Microwave Sensor With Highly Confined Fields for Aqueous-Glucose and Blood-Glucose Measurements," in IEEE Transactions on Instrumentation and Measurement, vol. 70, pp. 1-9, 2021, Art no. 8000309

[24] R. S. Hassan, "Wireless and battery-free biosensor based on parallel resonators for monitoring a wide range of biosignals," *IEEE Trans. Microw. Theory Techn.*, vol. 70, no. 10, pp. 4566–4578, Oct. 2022.

[25] Z. Yi and C. Wang, "Noninvasive glucose sensors using defective-ground-structure coplanar waveguide," *IEEE Sensors J.*, vol. 23, no. 1, pp. 195–201, Jan. 1, 2023.

[26] A. Kumar, *et al.*, "High-sensitivity, quantified, linear and mediator-free resonator-based microwave biosensor for glucose detection," *Sensors*, vol. 20, no. 14, Art. no. 4024, Jul. 2020.

[27] K. K. Adhikari and N.-Y. Kim, "Ultrahigh-sensitivity mediator-free biosensor based on a microfabricated microwave resonator for the detection of micromolar glucose concentrations," *IEEE Trans. Microw. Theory Techn.*, vol. 64, no. 1, pp. 319–327, Jan. 2016.

[28] M. Abdolrazzaghi, N. Katchinskiy, A. Y. Elezzabi, P. E. Light, and M. Daneshmand, "Noninvasive glucose sensing in aqueous solutions using an active split-ring resonator," *IEEE Sensors J.*, vol. 21, no. 17, pp. 18742–18755, Sept. 1, 2021.

[29] N. Kazemi and P. Musilek, "Enhancing microwave sensor performance with ultrahigh-Q features using CycleGAN," *IEEE Trans. Microw. Theory Techn.*, vol. 70, no. 12, pp. 5369–5382, Dec. 2022, doi: 10.1109/TMTT.2022.3218015.

Amjad Hussein Yousif is a Ph.D. senior (candidate) in electrical engineering with a research focus on microwave science and its sensing/communication applications. He earned his B.Sc. in Communication Engineering from Nineveh University in 2007, then completed a Higher Diploma in Electronics and Communication at the Electrical Engineering Department, College of Engineering, University of Mosul, in 2015. He went on to receive his M.Sc. in Electrical Engineering from the same department and college at the University of Mosul in 2022. His current interests span microwave resonators and sensors, RF/microwave circuit design, and non-invasive biomedical measurement techniques.

Saad Wasmi Osman Luhaib received the B.Sc. and M.Sc. degrees in Electronic and Communication Engineering from the University of Mosul, Iraq, in 2004 and 2007, respectively, and the Ph.D. degree in Communication Engineering from the University of Leeds, U.K., in 2018. He is currently an Assistant Professor with the Department of Electrical Engineering, University of Mosul. His research interests include microwave engineering, antennas, filters, multimode resonators, and communication systems.

Mohammed Younis Thanoun (*Member, IEEE*) received the Ph.D. degree in Communication Engineering/Computer Networks from the University of Mosul, Mosul, Iraq, in 2011. He is currently an Assistant Professor with the Department of Electrical Engineering, College of Engineering, University of Mosul. His research interests include deep learning applications in computer networks, network security, and communication engineering.